ARCHIVES OF ELECTRICAL ENGINEERING VOL. 61(3), pp. 389-410 (2012)

DOI 10.2478/v10171-012-0031-1

Dynamic variables limitation for backstepping control of induction machine and voltage source converter

MARCIN MORAWIEC

Gdansk University of Technology
Department of Automatic Control of Electrical Drives
e-mail: mmorawiec@ely.pg.gda.pl

(Received: 16.03.2012, revised: 21.05.2012)

Abstract: The paper presents the method of control of an induction squirrel-cage machine supplied by a voltage source converter. The presented idea is based on an innovative method of the voltage source converter control, consisting in direct joining of the motor control system with the voltage source rectifier control system. The combined control system gives good dc-bus voltage stabilization. In the applied control system the limits of the reference variables have been introduced. A correction of the estimated machine load torque is proposed. The new proposed solutions are confirmed by mathematical dependences, simulation and experimental results.

Key words: power electronics converters, backstepping control, dynamic variables limitation

1. Introduction

The voltage source converter is now one of the most popular converter systems transforming DC voltage into AC voltage. The industrial applications are most often based on the unidirectional voltage source inverter, where diode rectifier is installed on the supply network side. Such system has a large capacitance (of an order of several mF) capacitor in the dc-link circuit and the surplus of energy accumulated in it must be used up by the load or unloaded in a braking resistor.

Another solution is a bidirectional voltage source converter. Such system allows direct return of energy from the receiver to the supply network and also allows to achieve a unitary input power factor. The current input from the supply network may be close (in respect of the harmonic components) to the sinusoidal current. The dc-link circuit condenser has a several times smaller capacitance (depending on the load power) than that in the unidirectional voltage converter. Besides, the capacitor voltage can be stabilized, by means of a network voltage converter, at a higher value and therefore at the rated machine speed the converter can generate the appropriate stator voltage amplitude (the overmodulation range is not exceeded).

The dc-link filter can be optimized. With the use of an appropriate voltage source rectifier control system, the capacitor capacitance value can be decreased by several orders of magnitude. The properly performed voltage source converter optimization reduces the system size and also improves the drive system dynamic and static properties, lowering the production costs.

The solutions quoted in the literature [1-9] pertain to the voltage source rectifier control, are concentrated mainly on maintaining constant voltage in the dc-link circuit and on regulation of the active and reactive power on the supply network side. References [5, 8] present a control method based on the direction of the reference system in relation to the supply network virtual flux vector. In [5] a feedforward-based rectifier converter control method is presented. In [5, 9] a voltage source rectifier prediction control is applied.

The above mentioned reference papers deal with the bidirectional voltage source converter control, where the voltage source rectifier is used for voltage control in the dc-link circuit and for power control on the supply network side. The voltage source rectifier and motor converter control systems are mutually independent, linked only by the dc-link voltage, which should not exceed a 10% oscillation range. The mutual independence of network and motor converters has an impact on the dc-link voltage changes. In such control systems a higher capacitance condenser is necessary in the dc-link circuit.

The paper presents a new control system of voltage source rectifier where the backstepping [10-24] method is used. Through an appropriate formulation of the mathematical model of the drive system with an induction squirrel-cage motor, the machine mathematical model variables have been introduced to the voltage source rectifier control system. The combined coupling control system allows to minimize dc-link voltage balancing or minimize dc-link capacitors significantly.

The adaptive backstepping control for the induction machine was presented in [12-14, 25-26]. Authors of [12] compared standard Field Oriented Control (based on PI controllers) with the adaptive backstepping controller.

In this paper the multi-scalar [9, 14] adaptive backstepping control has been applied to the induction squirrel-cage machine. A new method of limiting the control system set variables has been applied. The control system of induction machine and voltage source rectifier with new multi-scalar backstepping controller and method of limiting allows to good quality drive performance which are shown in simulation and experimental results.

2. Mathematical models

A) Mathematical model of an induction machine

Equations of the induction squirrel-cage machine, written in a stationary ($\alpha\beta$) system, have the following form [9]:

$$\frac{di_{s\alpha}}{d\tau} = -\frac{R_s L_r^2 + R_r L_m^2}{L_r w_\sigma} i_{s\alpha} + \frac{R_r L_m}{L_r w_\sigma} \psi_{r\alpha} + \omega_r \frac{L_m}{w_\sigma} \psi_{r\alpha} + \frac{L_r}{w_\sigma} u_{s\alpha}, \tag{1}$$

$$\frac{di_{s\beta}}{d\tau} = -\frac{R_s L_r^2 + R_r L_m^2}{L_r w_\sigma} i_{s\beta} + \frac{R_r L_m}{L_r w_\sigma} \psi_{r\beta} - \omega_r \frac{L_m}{w_\sigma} \psi_{r\alpha} + \frac{L_r}{w_\sigma} u_{s\beta}, \tag{2}$$

$$\frac{d\psi_{r\alpha}}{d\tau} = -\frac{R_r}{L_r} \psi_{r\alpha} - \omega_r \psi_{r\beta} + \frac{R_r L_m}{L_r} i_{s\alpha}, \tag{3}$$

$$\frac{d\psi_{r\beta}}{d\tau} = -\frac{R_r}{L_r} \psi_{r\beta} + \omega_r \psi_{r\alpha} + \frac{R_r L_m}{L_r} i_{s\beta}, \tag{4}$$

$$\frac{d\omega_r}{d\tau} = \frac{L_m}{J L_r} \left(\psi_{r\alpha} i_{s\beta} - \psi_{r\beta} i_{s\alpha} \right) - \frac{1}{J} T_L, \tag{5}$$

where: $i_{s\alpha}$, $i_{s\beta}$ are components of the stator current vector, $\Psi_{r\alpha}$, $\Psi_{r\beta}$ are components of the rotor flux vector, $u_{s\alpha}$, $u_{s\beta}$ are components of the stator voltage vector, ω_r is the rotor angular speed, R_r, R_s are the rotor and stator resistances, L_m is the mutual-flux inductance, L_s, L_r are the stator and rotor inductances, $w_\sigma = L_r L_s - L_m^2$, T_L is a load torque, J is the machine moment of inertia, τ is the relative time.

B) Mathematical model of the supply network

The supply network mathematical model, in the system connected with the supply network voltage vector (dq), takes the following form:

$$\frac{di_{cd}}{d\tau} = \frac{1}{L} \left(v_s - R i_{cd} + \omega_u L i_{cq} - u_d \right), \tag{6}$$

$$\frac{di_{cq}}{d\tau} = \frac{1}{L} \left(-R i_{cq} - \omega_u L i_{cd} - u_q \right), \tag{7}$$

where: L is the system input choking coil inductance, R is the choking coil internal resistance, i_{cd}, i_{cq} are components of the network current vector in the network voltage-related system, u_d, u_q are components of the voltage source rectifier input voltage (control variables of VSR), ω_u is the supply network voltage vector rotation speed. The supply network parameters are presented in Table 1 in p.u.

3. Voltage source rectifier control

A) The controller based on Lyapunov Function CLF

The voltage source rectifier may be treated as a voltage stabilizing system in the dc-link. In drive systems with a diode rectifier a large capacitance is needed in the converter dc-link. In drive systems with a voltage source converter the capacitor capacitance may be minimized.

For determination of the voltage source rectifier control variables $\left(u_d^*, u_q^*\right)$ the *Lyapunov* method (CLF – *Control Lyapunov Function*) may be used, as presented in [17]. In order to

determine the control system stabilizing feedbacks, the network current deviations have been defined (in accordance with a classic voltage source rectifier control scheme):

$$e_1 = u_{dc}^* - u_{dc}, \tag{8}$$

$$e_2 = i_{cd}^* - i_{cd}, \tag{9}$$

$$e_3 = i_{cq}^* - i_{cq}, \tag{10}$$

where: i_{cd}^* is the value obtained from the dc bus voltage controller.

The network current deviation derivatives are determined as follows:

$$\dot{e}_2 = \frac{d}{d\tau} i_{cd}^* - \frac{1}{L}\left(v_s - Ri_{cd} + \omega_u L i_{cq} - u_d^*\right), \tag{11}$$

$$\dot{e}_3 = \frac{d}{d\tau} i_{cq}^* - \frac{1}{L}\left(-Ri_{cq} - \omega_u L i_{cd} - u_q^*\right). \tag{12}$$

In accordance with the Lyapunov method, the following function is selected:

$$V = \frac{1}{2}\left(k_2 e_2^2 + k_3 e_3^2\right). \tag{13}$$

Substituting (11)-(12) to(13), one obtains:

$$\begin{aligned} \dot{V} = -k_2 e_2^2 - k_3 e_3^2 + e_2\left[-\frac{1}{L}\left(v_{sieć} - Ri_{cd} + \omega_u L i_{cq} - u_d^*\right) + k_2 e_2\right] + \\ + e_3\left[k_3 e_3 - \frac{1}{L}\left(-Ri_{cq} - \omega_u L i_{cd} - u_q^*\right)\right]. \end{aligned} \tag{14}$$

The control variables are determined from (14):

$$u_d^* = v_s - Ri_{cd} + L\left(\omega_u i_{cq} - k_2 e_2\right), \tag{15}$$

$$u_q^* = -Ri_{cq} - L\left(\omega_u i_{cd} + k_3 e_3\right), \tag{16}$$

where: k_1, k_2 – amplification constants.

The (15)-(16) control variables linearize the system and ensure stabilization around the equilibrium point.

The control system is little resistant to the load torque changes. Lack of the machine load torque information may cause instantaneous dc-link voltage oscillations.

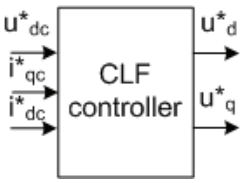

Fig. 1. Standard CLF controller without feedforward

B) The backstepping controller

Coupling of the motor control and voltage source rectifier control systems allows better dc-link voltage control and the dc-link capacitance minimization. For coupling the control system – the backstepping control was used (presented, a.o., in [10-24]).

The voltage source rectifier control system should ensure stabilization of the dc-link voltage at a constant value and maintain the network current vector set component as proportional to the reactive power on the supply network side.

The current flowing from the capacitor to the machine may be defined as:

$$i_{sil} = \frac{p_{sil}}{u_{dc}}, \tag{17}$$

where: p_{sil} is the active power measured on the machine phase terminals.

The current flowing to the capacitor is defined as:

$$i_{dconv} = \frac{p_{conv}}{u_{dc}}, \tag{18}$$

where: p_{conv} is the active power measured on the voltage source rectifier input.

The following relation is fulfilled for the dc-link:

$$\frac{du_{dc}}{d\tau} = \frac{1}{Cu_{dc}}\left(p_{conv} - p_{sil}\right). \tag{19}$$

The e_1 deviation derivative is determined by the formula:

$$\dot{e}_1 = \dot{u}_{dc}^* - \frac{1}{C}\left(i_{conv} - i_{sil}\right). \tag{20}$$

On the assumption that component $i_{cq}^* \approx 0$, the i_{conv} current flowing into the dc-link capacitor is equal to: $i_{conv} \approx i_{cd}$.

In order to achieve the control variables $\left(u_d^*, u_q^*\right)$, the backstepping approach is implemented.

Selecting the Lyapunov function for the first subsystem where virtual control was sought, the following expression was obtained:

$$\dot{V} = k_1 e_1 + \dot{u}_{dc}^* - \frac{1}{C}\left(i_{cd} - i_{sil}\right). \tag{21}$$

The virtual control obtained from (21) takes the form:

$$i_{cd}^* = Ck_1 e_1 + \dot{u}_{dc}^* C + i_{sil}. \tag{22}$$

With the use of (22), the e_2 deviation becomes:

$$e_2 = Ck_1 e_1 + \dot{u}_{dc}^* C + i_{sil} - i_{cd} \tag{23}$$

and the deviation e_1 derivative is modified correspondingly:

$$\dot{e}_1 = -k_1 e_1 + \frac{1}{C} e_2 . \tag{24}$$

The deviation e_2 derivative takes the form:

$$\dot{e}_2 = Ck_1 \dot{e}_1 + \dot{u}_{dc}^{*} C + \dot{i}_{sil} - \dot{i}_{cd} . \tag{25}$$

In the above expression appears the derivative of current flowing from the dc-link capacitor, $\dot{i}_{sil}$. The current derivative was obtained by differentiation of the (17) formula and it takes the following form:

$$\frac{di_{sil}}{d\tau} = -i_{sil}\left(a_1 - \frac{1}{u_{dc} C}\left(i_{sil} - i_{cd}\right)\right) + a_2 \frac{G_{11}}{u_{dc}} + a_3 x_{11} \frac{G_{22}}{u_{dc}} + a_4 \frac{u_s^2}{u_{dc}} + \frac{1}{u_{dc}^2}\left(\dot{u}_{s\alpha} i_{s\alpha} + \dot{u}_{s\beta} i_{s\beta}\right), \tag{26}$$

where:

$$G_{11} = \psi_{r\alpha} u_{s\alpha} + \psi_{r\beta} u_{s\beta}, \quad G_{22} = \psi_{r\beta} u_{s\alpha} - \psi_{r\alpha} u_{s\beta}, \quad u_s^2 = u_{s\alpha}^2 + u_{s\beta}^2$$

and

$$a_1 = \frac{R_s L_r^2 + R_r L_m^2}{L_r w_\sigma}, \quad a_2 = \frac{R_r L_m}{L_r w_\sigma}, \quad a_3 = \frac{L_m}{w_\sigma}, \quad a_4 = \frac{L_r}{w_\sigma}.$$

For determination of the (26) derivative the mathematical model of an induction machine (1)-(5) was used.

The expression $\dot{u}_{s\alpha} i_{s\alpha} + \dot{u}_{s\beta} i_{s\beta}$ in (26) can be presented in the form:

$$\dot{u}_{s\alpha} i_{s\alpha} + \dot{u}_{s\beta} i_{s\beta} = \frac{du_s}{d\tau} i_{sd} + \omega_{us} q_s , \tag{27}$$

where: u_s is the machine stator voltage modulus, ω_{us} is the stator voltage vector rotation speed, i_{sd} is the stator current component in the coordinate system oriented in accordance with the stator voltage vector,

$$q_s = -u_{s\beta} i_{s\alpha} + u_{s\alpha} i_{s\beta} , \tag{28}$$

is the reactive power defined on the machine side.

The (27) formula may be simplified by assumption that the machine voltage modulus is a slow-changing signal and its derivative is close to zero:

$$\frac{du_s}{d\tau} \approx 0. \tag{29}$$

Taking (29) into account, (27) becomes:

$$\dot{u}_{s\alpha} i_{s\alpha} + \dot{u}_{s\beta} i_{s\beta} = \omega_{us} q_s . \tag{30}$$

With the above simplification, (26) is now:

$$\frac{di_{sil}}{d\tau}=\frac{1}{u_{dc}}\left(a_2G_{11}+a_3x_{11}G_{22}+a_4u_s^2\right)+\frac{1}{u_{dc}^2}\omega_{us}q_s-i_{sil}\left(a_1-\frac{1}{u_{dc}C}\left(i_{sil}-i_{cd}\right)\right). \tag{31}$$

Substituting the derivative of the motor current modulus to the deviation derivative expression, one obtains:

$$\begin{aligned}\dot{e}_2=Ck_1\left(-k_1e_1+\frac{1}{C}e_2\right)+\frac{1}{u_{dc}}\left(a_2G_{11}+a_3x_{11}G_{22}+a_4u_s^2\right)+\\+\frac{1}{u_{dc}^2}\omega_{us}q_s-i_{sil}\left(a_1-\frac{1}{u_{dc}C}\left(i_{sil}-i_{cd}\right)\right)-\frac{1}{L}\left(v_s-Ri_{cd}+\omega_uLi_{cq}-u_d^*\right).\end{aligned} \tag{32}$$

For the second subsystem responsible for maintaining the set value of reactive power, the expression (12) is valid.

The Lyapunov function is selected as follows:

$$V=\frac{1}{2}\left(k_1e_1^2+k_2e_2^2+k_3e_3^2\right). \tag{33}$$

The Lyapunov function derivative has the form:

$$\begin{aligned}\dot{V}=-(k_2e_2^2+k_3e_3^2)+e_2[k_2e_2+\frac{1}{C}e_1-Ck_1^2e_1+k_1e_2+\frac{1}{u_{dc}}(a_2G_{11}+a_3x_{11}G_{22}+a_4u_s^2)+\\-i_{sil}(a_1-\frac{1}{u_{cd}C}(i_{sil}-i_{cd}))+\frac{1}{u_{dc}^2}\omega_{us}q_s-\frac{1}{L}(v_s-Ri_{cd}+\omega_uLi_{cq}-u_d^*)]+\\+e_3\left(k_3e_3-\frac{1}{L}(-Ri_{cq}-\omega_uLi_{cd}-u_q^*)\right).\end{aligned} \tag{34}$$

By introducing new f_1 and f_2 variables, the voltage source rectifier control variables were obtained:

$$u_d^*=-Lf_1, \tag{35}$$

$$u_q^*=-Lf_2, \tag{36}$$

where:

$$\begin{aligned}f_1=limit_u\cdot\left(-Ck_1^2+\frac{1}{C}\right)e_1+k_2e_2+k_1e_2+\frac{1}{u_{dc}^2}\omega_{us}q_s-i_{sil}\left(a_1-\frac{1}{u_{dc}C}i_{sil}+\frac{1}{u_{dc}C}i_{cd}\right)+\\-\frac{1}{L}\left(v_s-Ri_{cd}+\omega_uLi_{cq}\right)+\frac{1}{u_{dc}}\left(a_2G_{11}+a_3x_{11}G_{22}+a_4u_s^2\right),\end{aligned} \tag{37}$$

$$f_2=\left(k_3e_3+\frac{R}{L}i_{cq}+\omega_ui_{cd}\right), \tag{38}$$

where: $limit_u$ allows to limit the dynamics of the i^*_d component (Chapter 5).

The above formulae were obtained for an induction machine supplied from a voltage source converter. In the proposed backstepping control the control variables depend on the load type. The above given formulae are valid for a squirrel-cage induction machine supplied from a voltage source converter. If the voltage source converter is loaded by another machine, e.g. a synchronous machine with permanent magnets, the stator current derivative must be adequately defined using the mathematical model of a synchronous motor.

4. The multi-scalar backstepping control of induction machine

A) Adaptive backstepping control with load torque estimation

The backstepping control can be appropriately written for an induction squirrel-cage machine supplied from a voltage source converter. In literature the backstepping control is known with adaptation of selected machine parameters, written for an induction motor [10-24]. In [10-14, 16-24] the authors wrote the machine state variables in the (dq) coordinate system, oriented in accordance with the rotor flux vector (FOC). The control method presented in [10-14, 16-24] is based on control of the motor state variables: ω_r – rotor angular speed, rotor flux modulus and the stator current vector components: i_{sd} and i_{sq}.

Selection of the new motor state variables, as in the case of multi-scalar control with linear PI regulators [9, 13], leads to a different form of expressions describing the machine control and decoupling. The following state variables have been selected for the multi-scalar backstepping control:

$$e_1 = x_{11}^* - x_{11}, \tag{39}$$

$$e_2 = x_{12}^* - x_{12}, \tag{40}$$

$$e_3 = x_{21}^* - x_{21}, \tag{41}$$

$$e_4 = \left(2R_r \frac{L_m}{L_r} x_{22}\right)^* - 2R_r \frac{L_m}{L_r} x_{22}, \tag{42}$$

where: x_{11} is the rotor speed, x_{12} is the electromagnetic moment, x_{21} is the square of rotor flux, x_{22} is an additional variable.

Assumption of such machine state variables may lead to improvement of the control system quality due to the fact that e.g. the x_{12} variable is directly the electromagnetic torque of the machine. In [10-14, 16-24] the electromagnetic moment is not directly but indirectly controlled (the i_{sq} stator current component). With the assumption of a constant rotor flux modulus, such a control conception is correct. The inaccuracy of the machine parameters, asymmetry or inadequately aligned control system may lead to couplings between control circuits. Acceptance of the control deviations as in (39)-(42) increases the control system resistance to the described phenomena.

The e_4 deviation is defined in (42). The deviation does not influence on the control system properties and is only an accepted simplification in the format of decoupling variables.

Derivatives of the (39)-(42) deviations take the form:

$$\dot{e}_1 = \frac{L_m}{JL_r} e_2 - k_1 e_1 - \frac{\tilde{T}_L}{J}, \tag{43}$$

$$\dot{e}_2 = -k_1^2 e_1 \frac{JL_r}{L_m} + k_1 e_2 + a_1 x_{12} + x_{11}\left(x_{22} + \frac{L_m}{w_\sigma} x_{21}\right) - k_1 \frac{L_r}{L_m}\tilde{T}_L + \frac{L_r}{L_m}\dot{\hat{T}}_L - \frac{L_r}{w_\sigma} u_1, \tag{44}$$

$$\dot{e}_3 = -k_3 e_3 + e_4, \tag{45}$$

$$\begin{aligned}\dot{e}_4 = {} & -k_3^2 e_3 + k_3 e_4 - 4\left(\frac{R_r}{L_r}\right)^2 x_{21} + 4L_m\left(\frac{R_r}{L_r}\right)^2 x_{22} + 2\frac{R_r L_m}{L_r} a_1 x_{22} - 2\frac{R_r L_m}{L_r} x_{11} x_{22} + \\ & - \frac{2}{w_\sigma}\left(\frac{R_r L_m}{L_r}\right)^2 x_{21} - 2\left(\frac{R_r L_m}{L_r}\right)^2 i_s^2 - 2\frac{R_r L_m}{w_\sigma} u_2,\end{aligned} \tag{46}$$

where

$$\tilde{T}_L = \hat{T}_L - T_L. \tag{47}$$

The reference values of x_{12} and x_{22} are determined by

$$\hat{x}_{12}^* = \frac{JL_r}{L_m} k_1 e_1 + \frac{L_r}{L_m}\hat{T}_L, \quad \left(2R_r \frac{L_m}{L_r} x_{22}\right)^* = k_3 e_3 + 2\frac{R_r}{L_r} x_{21}. \tag{48}$$

$$\left(2R_r \frac{L_m}{L_r} x_{22}\right)^* = k_3 e_3 + 2\frac{R_r}{L_r} x_{21}. \tag{49}$$

The Lyapunov function derivative, with (43)-(46) taken into account, is expressed as follows:

$$\begin{aligned}\dot{V} = {} & -k_1 e_1^2 - k_2 e_2^2 - k_3 e_3^2 - k_4 e_4^2 - \frac{1}{\gamma}\tilde{T}_L\dot{\tilde{T}}_L + e_2\left(f_1 - \frac{L_r}{w_\sigma} u_1\right) + e_4\left(f_2 - 2\frac{R_r L_m}{w_\sigma} u_2\right) + \\ & + \tilde{T}_L\left(\frac{1}{\gamma}\dot{\hat{T}}_L - \frac{e_1}{J} - k_1 \frac{L_r}{L_m} e_2\right),\end{aligned} \tag{50}$$

$$f_1 = k_1 e_2 + k_2 e_2 + limit_{12} \cdot \left(\frac{L_m}{JL_r} e_1 - k_1^2 e_1 \frac{JL_r}{L_m}\right) + a_1 x_{12} + x_{11}\left(x_{22} + \frac{L_m}{w_\sigma} x_{21}\right) + \frac{L_r}{L_m}\dot{\hat{T}}_L, \tag{51}$$

$$\begin{aligned}f_2 = {} & k_4 e_4 + k_3 e_4 + limit_{22} \cdot \left(e_3 - k_3^2 e_3\right) - 4\left(\frac{R_r}{L_r}\right)^2 x_{21} + 4L_m\left(\frac{R_r}{L_r}\right)^2 x_{22} + 2\frac{R_r L_m}{L_r} a_1 x_{22} + \\ & - 2\frac{R_r L_m}{L_r} x_{11} x_{22} - \frac{2}{w_\sigma}\left(\frac{R_r L_m}{L_r}\right)^2 x_{21} - 2\left(\frac{R_r L_m}{L_r}\right)^2 i_s^2,\end{aligned} \tag{52}$$

where: $u_1 = \psi_{r\alpha} u_{s\beta} - \psi_{r\beta} u_{s\alpha}$, $u_2 = \psi_{r\alpha} u_{s\alpha} - \psi_{r\beta} u_{s\beta}$, $limit_{12}$ – is a dynamic limitation in the motor speed control subsystem, $limit_{22}$ – is a dynamic limitation in the rotor flux control subsystem.

The control variables take the form:

$$u_{s\alpha}^{*} = \frac{L_r \psi_{r\alpha} f_2 - w_\sigma a_3 \psi_{r\beta} f_1}{a_3 L_r x_{21}}, \tag{53}$$

$$u_{s\beta}^{*} = \frac{L_r \psi_{r\beta} f_2 + w_\sigma a_3 \psi_{r\alpha} f_1}{a_3 L_r x_{21}}, \tag{54}$$

where:

$$a_3 = 2\frac{R_r L_r}{w_\sigma}.$$

The load torque T_L can be estimated from the formula:

$$\dot{\hat{T}}_L = \gamma \left(\frac{e_1}{J} + k_1 \frac{L_r}{L_m} e_2 \right), \tag{55}$$

where: γ is a constant gain.

The variables $limit_{12}$, $limit_{22}$ in (51) and (52) are defined in Chapter 5 as limitation of $\hat{x}_{12}^{*}$ and $\hat{x}_{22}^{*}$ property.

5. Dynamic limitations of the set variables

In control systems with the conventional linear controllers of the PI or PID type, the set (or controller output) variable dynamics are limited to a constant value or dynamically changed, depending on the drive working point.

Control systems where the control variables are determined from the Lyapunov function have no limitations in the set variable control circuits. The reference variable dynamics may be limited by means of additional first order inertia elements.

The author of this paper has not come across a solution of the problem in the most significant backstepping control literature references, e.g. [10-24]. In the quoted reference positions, the authors propose the use of inertia elements on the set variable signals. Such approach is an intermediate method, not giving any rational control effects. The use of an inertia element on the reference signal, e.g. of the rotor angular speed, will slow down the reference electromagnetic torque reaction in proportion to the inertia element time-constant. In effect a "slow" build-up of the motor electromagnetic torque is obtained, which may be acceptable in some applications. In practice the aim is to limit the electromagnetic torque value without an impact on the build-up dynamics.

Control systems with the Lyapunov function-based control without limitation of the set variables are not suitable for direct adaptation in the drive systems. Therefore, a solution often quoted in literature, e.g. in [17], is the use of a PI or PID speed controller at the moment control circuit input.

The set values of the x_{12}^*, x_{22}^* variables appearing in the e_2 and e_4 deviations can be dynamically limited and the dynamic limitations are defined by the expressions [13]:

$$x_{12lim} = \sqrt{I_{smax}^2 x_{21} - x_{22}^2}, \tag{56}$$

$$x_{22lim} = f\left(U_{smax}^2, I_{smax}^2, x_{11}\right), \tag{57}$$

where: x_{12lim} – the set moment limitation, x_{22lim} – the x_{22} variable limitation, I_{smax} – maximum value of the stator current modulus, U_{smax} – maximum value of the stator voltage modulus.

The above given expressions may be modified to the form [26]:

$$x_{12lim} = \sqrt{I_{smax}^2 x_{21} - \frac{x_{21}^2}{L_m^2}}, \tag{58}$$

giving the relationship between the x_{21} variable, the stator current modulus I_{smax}, and the motor set moment limitation.

For the multi-scalar backstepping control, to the f_1 and f_2 variables the $limit_{12}$ and $limit_{22}$ variables were introduced; they assume the 0 or 1 value depending on the need of limiting the set variable.

Limitation of variables in the Lyapunov function-based control systems may be performed in the following way:

$$if\ \left(x_{12}^* > x_{12lim}\right)\ \text{then}\ \left\{\begin{matrix} limit_{12} = 0, \\ e_2 = x_{12lim} - x_{12} \end{matrix}\right\}, \tag{59}$$

$$if\ \left(x_{12}^* < -x_{12lim}\right)\ \text{then}\ \left\{\begin{matrix} limit_{12} = 0, \\ e_2 = -x_{12lim} - x_{12} \end{matrix}\right\},\ \text{else}\ limit_{12} = 1, \tag{60}$$

$$\text{if}\ \left(x_{22}^* > x_{22lim}\right)\ \text{then}\ \left\{\begin{matrix} limit_{22} = 0, \\ e_4 = x_{22lim} - x_{22} \end{matrix}\right\}, \tag{61}$$

$$\text{if}\ \left(x_{22}^* < -x_{22lim}\right)\ \text{then}\ \left\{\begin{matrix} limit_{22} = 0, \\ e_4 = -x_{22lim} - x_{22} \end{matrix}\right\},\ \text{else}\ limit_{22} = 1. \tag{62}$$

The dynamic limitations effected in accordance with expressions (59)-(62) limit properly the value of x_{12}^* and x_{22}^* variables without any interference in the reference signal build-up dynamics. The $limit_u$ variable in (37) assumes the 0 or 1 values. The $limit_u$ allows to limit the dynamics of the i_d^* component. The limitation is performed in a similar way as in (59)-(62).

Figure 2 presents the variable simulation diagrams. The backstepping control dynamic limitations were used.

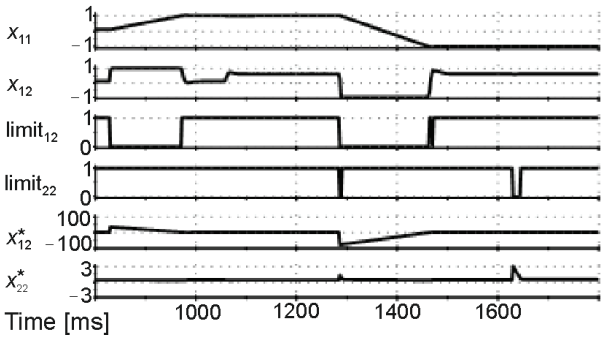

Fig. 2. Diagrams of multi-scalar variables in the machine dynamic states, the $x_{12ogr} = 1.0$ and $x_{22ogr} = 0.74$ limitations were set for a drive system with an induction squirrel-cage machine supplied from a voltage source converter – simulation diagrams, x^*_{12} – diagram of the machine set electromagnetic moment (no signal limitation), x^*_{22} – diagram of the x^*_{22} set signal (no limitation)

6. Impact of the dynamic limitation on the estimation of parameters

The use of a variable limitation algorithm may have a negative impact on the control system estimated parameters. This has a direct connection with the limited deviation values, which are then used in an adaptive parameter estimation. Such phenomenon is presented in Figure 2. The estimated parameter in the control system is the motor load torque $\hat{T}_L$. The set electromagnetic moment is limited to the $x_{12lim} = 1.0$ value. Figure 2 shows that the estimated load torque increases slowly in the intermediate states. Limitation of the set electromagnetic moment causes the limitation of deviation e_2, which in turn causes limited increase dynamics of the estimated load torque. The $\hat{T}_L$ value for $\text{limit}_{12} = 0$ in the dynamic states does not reach the real value of the load torque, which should be $\hat{T}_L \approx x_{12}$. A large $\hat{T}_L$ estimation error occurs in the intermediate states, which can be seen in Figure 3. The estimation error in the intermediate states is $\tilde{T}_L \neq 0$ because the moment limitation, introduced to the control system, is not compensated. The simulation and experimental tests have shown that the load torque estimation error in the intermediate state has an insignificant impact on the speed control. Omitting $\hat{T}_L$ in the set moment x^*_{12} expression (48) eliminates the intermediate state speed over-regulation. But absence of $\hat{T}_L$ in x^*_{12} for a steady state gives the deviation value $e_1 \neq 0$ and lack of full control over maintaining the rotor set angular speed. Compensation of the $limit_{12}$ limitation introduced to the control system is possible by installing a corrector in the rotor angular speed control circuit.

A corrector in the form of an e_1 signal integrating element was added to the set electromagnetic moment x^*_{12} signal. In this way a system was obtained reacting to the change of machine real load torque. The introduced correction minimizes the rotor angular speed deviation and the corrector signal may be treated as the estimated load torque value.

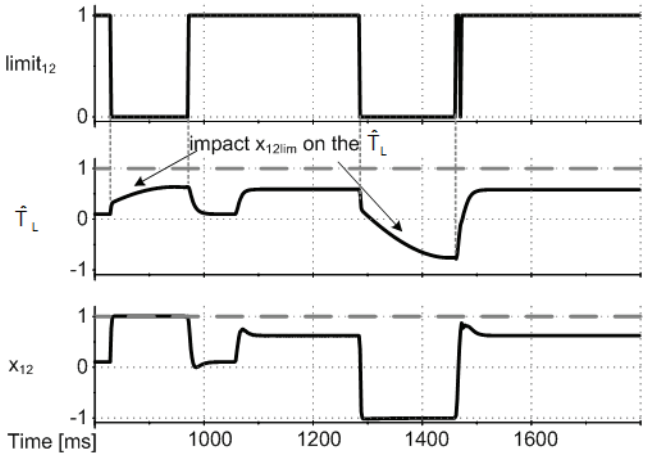

Fig. 3. Impact of the electromagnetic moment limitation x_{12lim} on the estimated load torque $\hat{T}_L$ (55)

The correction element is determined by the expression:

$$KT_L = k_{e1} \int_{t_{k-1}}^{t_k} e_1 d\tau \,, \tag{63}$$

where: $t_{k-1} \ldots t_k$ is the e_1 signal integration range, KT_L – correction element, k_{e1} – is the correction element amplification.

The gain k_{e1} should be adjusted that the speed overregulation in the intermediate state does not exceed 5%:

$$0 < k_{e1} \le 0{,}1 \cdot k_1 \,, \tag{64}$$

The correction element amplification must not be greater than k_1, or:

$$k_{e1} \le k_1 \tag{65}$$

For $k_{e1} > k_1$ the KT_L signal will become an oscillation element and may lead to the control system loss of stability.

The KT_L signal must be limited to the x_{12lim} value.

The x^*_{12} set value expression (48) must be modified:

$$x^*_{12} = \frac{JL_r}{L_m} k_1 e_1 + KT_L \,, \tag{66}$$

where:

$$\hat{T}_L \approx KT_L \,. \tag{67}$$

The use of (63) and (66) in the angular speed control circuit improves the load torque estimation and eliminates the steady state speed error.

Figure 4 presents the load torque (determined in (69)) estimation as well as x_{12} and the $limit_{12}$ limitations.

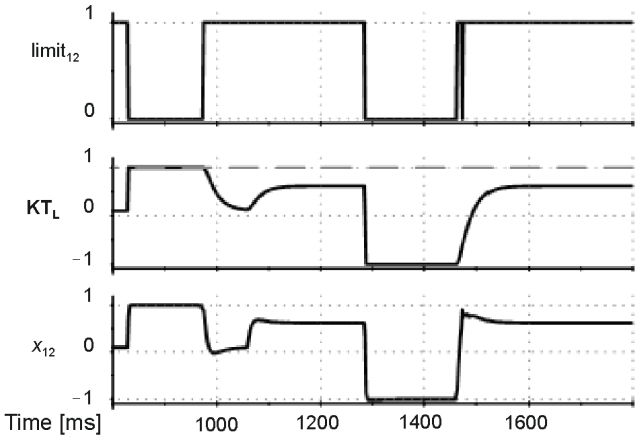

Fig. 4. Diagrams of the $limit_{12}$ variable, KT_L load torque and electromagnetic torque x_{12}

7. The speed observer backstepping

General conception of the adaptive control with backstepping is presented in references [11, 10]. In [11] the adaptive backstepping observer stability is proved and the stability range is given. The speed observer backstepping equations was presented in [28]. The rotor speed was estimated form dependence:

$$\dot{\hat{\omega}}_r = \gamma a_6 \left(z_\beta \hat{\psi}_{r\alpha} - z_\alpha \hat{\psi}_{r\beta} \right). \tag{68}$$

where: γ is constant amplifications.

Block diagram of a control system with the backstepping control and observer is shown in Figure 5.

8. Experimental results

The tests were carried out in a 160 kW drive system. The motor parameters are given in Table 1 and the main per unit values in Table 2. The control system was implemented in DSP Shark Sh363 signal processor with Altera Cyclon 2 FPGA. The transistor switching frequency was 3.3 kHz for both inverters.

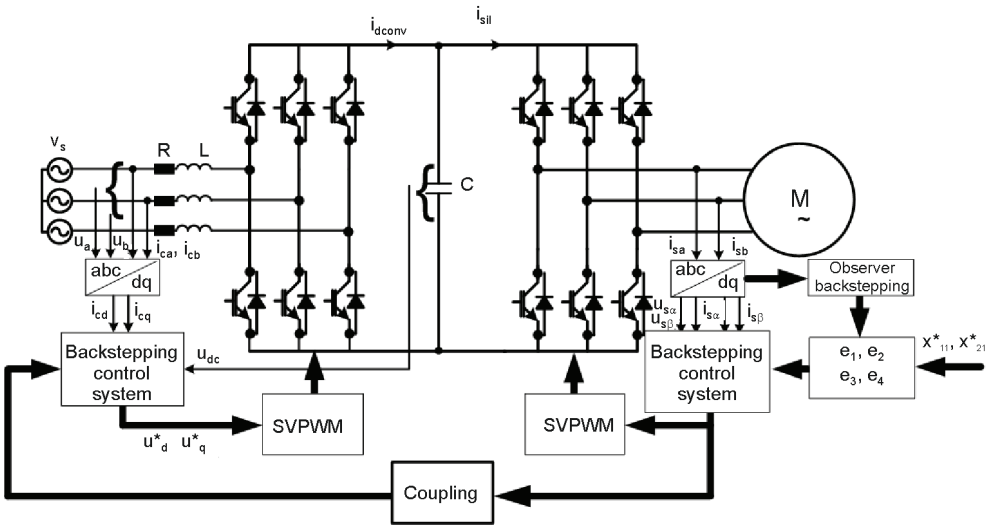

Fig. 5. The multi-scalar adaptive backstepping control system

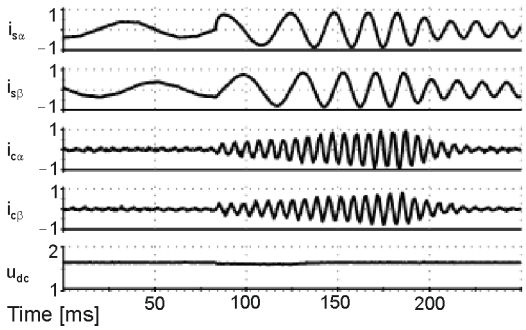

Fig. 6. Transient in motor start up to 0.8 p.u. in the backstepping control system

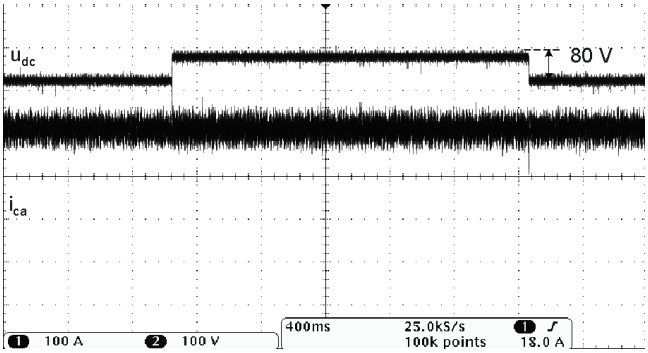

Fig. 7. u^*_{dc} is changed from 600 V to 680 V in the steady state

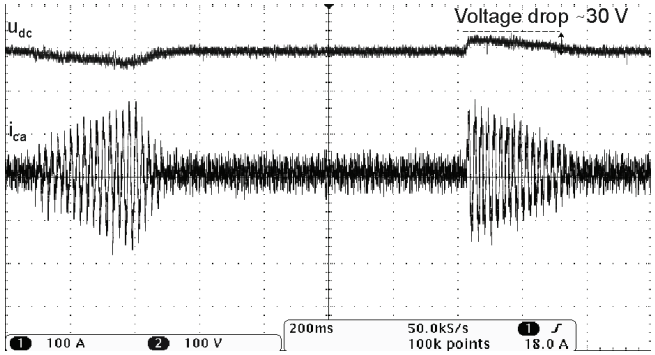

Fig. 8. Transient: motor start up to 0.8 p.u. and reversal to –0.8 p.u., u_{dc} voltage balance is ~5% – the backstepping control

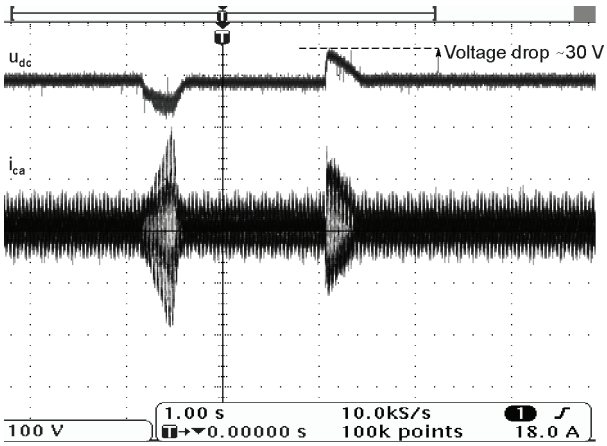

Fig. 9. Transient: motor start up to 0.8 p.u. and reversal to –0.8 p.u., u_{dc} voltage balance is ~13% – the CLF control with feedfoward coupling

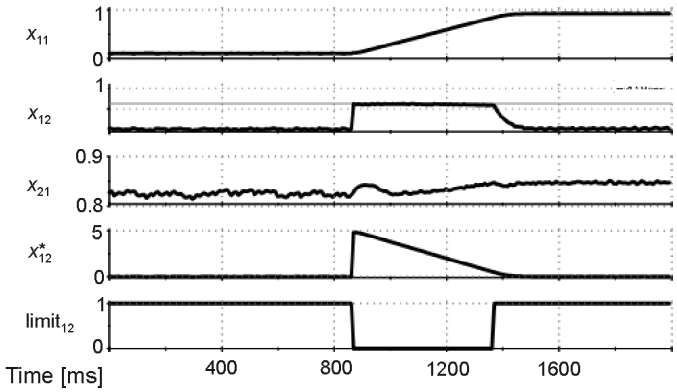

Fig. 10. Transient when motor is starting up to 0.95 p.u. without load torque estimation

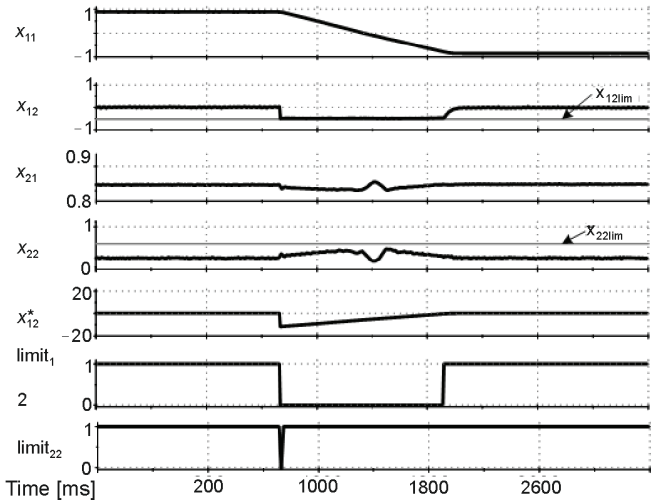

Fig. 11. Transients: motor reversal from 0.95 to –0.95 p.u. without load torque estimation, multi-scalar variables are shown and x^*_{12} is the (68) variable

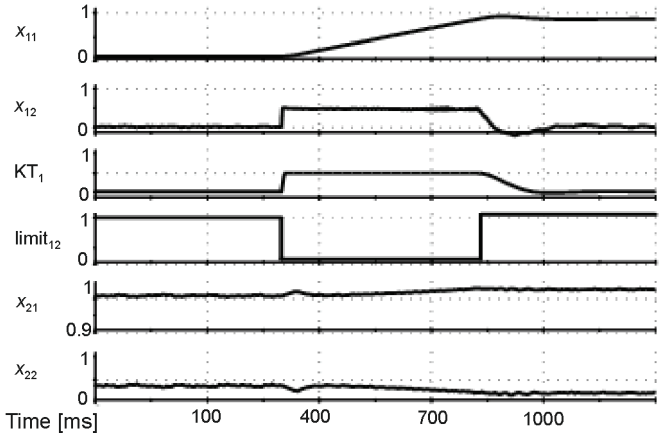

Fig. 12. Transient: motor start up to 0.9 p.u. with load torque estimation (KT_L) – the adaptive backstepping control

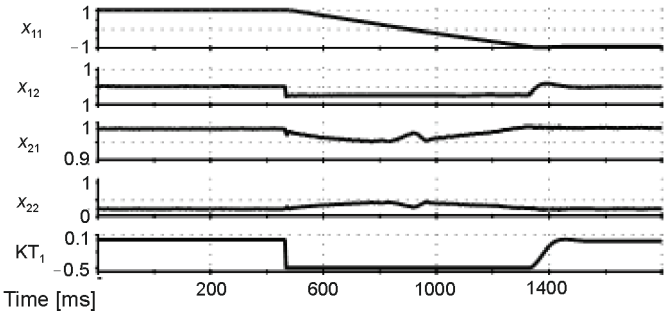

Fig. 13. Transients: motor reversal from 1.0 to – 1.0 p.u. with load torque estimation (KT_L)

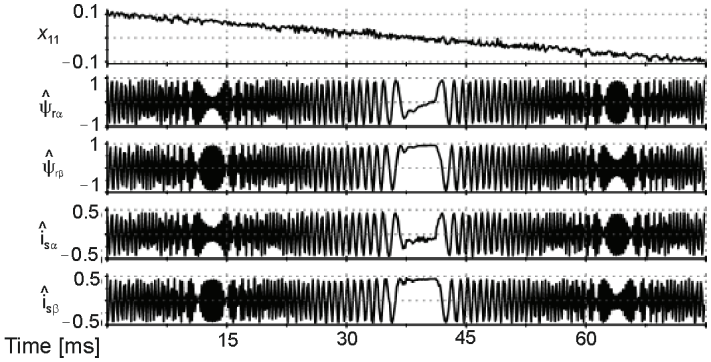

Fig. 14. Speed observer test: the rotor speed x_{11} is changed from 0.1 to −0.1 p.u., the rotor flux and stator current coefficients are shown

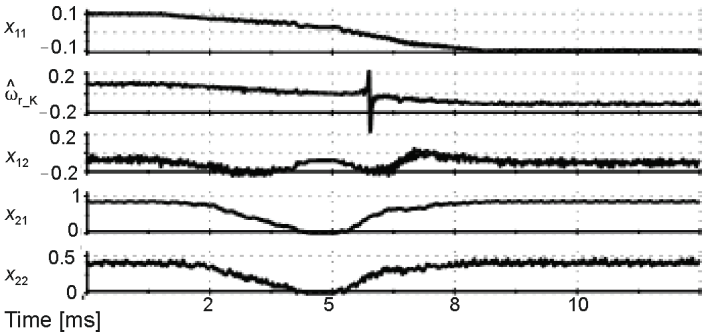

Fig. 15. The Speed observer test: the estimated rotor speed x_{11} in backstepping observer is changed from 0.1 to −0.1 p.u., the estimated rotor speed $\hat{\omega}_{r\_K}$ by Krzeminski's speed observer [27] and the multi-scalar variable: x_{12}, x_{21}, x_{22} are shown

The experimental results (Fig. 5, 9-13) were registered by measurement console. The reference speed was set-up from console without ramp time.

Figure 6 presents the stator current components as well as the supply network current and the dc-link voltage components during the motor start up to 0.8 p.u. speed. Figure 7 shows the change of dc-link voltage setting from 600 V to 680 V and the supply network current i_{ca}.

Figures 7 and 8 present the motor start up to 0.8 p.u. speed and motor reversal to −0.8 p.u. in the voltage source rectifier backstepping control system (Fig. 8) and the CLF system (Fig. 9). The voltage source rectifier backstepping control system better stabilises the dc-link voltage (Fig. 8). The u_{dc} voltage variation for the CLF system is about 80 V and for the backstepping control system about 30 V (Fig. 9). Figure 10 and 11 present diagrams of the machine multiscalar variables as well as the motor start-up (Fig. 10) and reversal (Fig. 11) limitations. The use of control without the load torque estimation results in small intermediate state speed error (Fig. 10, 11) and 7% steady state speed error. Figures 12 and 13 present the motor start-up and reversal. The use of the load torque estimation according to the (65) expression allows to minimise the steady state speed error. The speed error in the intermediate states is <2%. Figure 14 presents a 60 s machine reversal from the 0.1 to −0.1 p.u. speed.

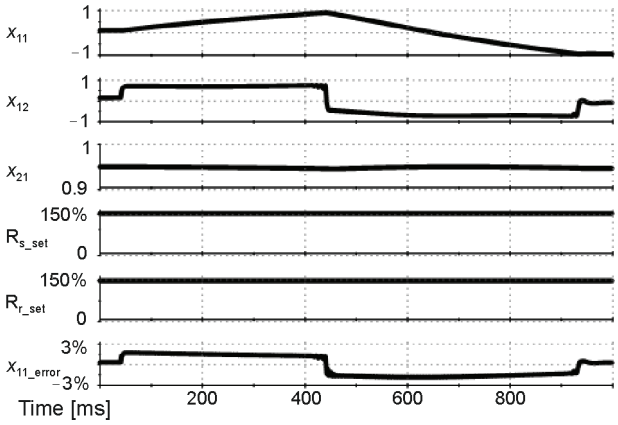

Fig. 16. Stator resistance R_{s_set} and R_{r_set} are change about 150% when rotor speed is set up to 1.0 and after 430ms to −1.0 p.u. (simulation results). The parameters are not estimated

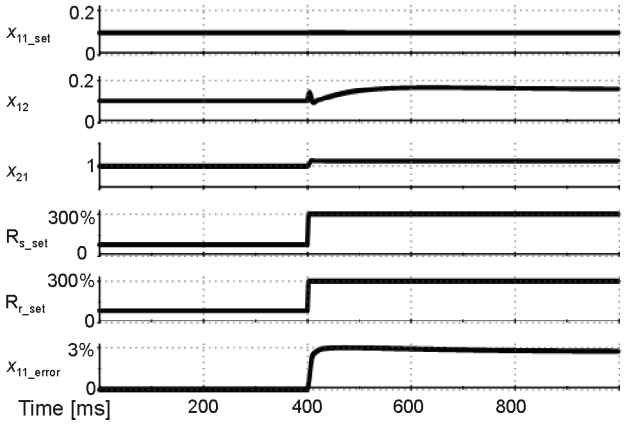

Fig. 17. Stator resistance R_{s_set} and R_{r_set} are change about 300% in stationary state (simulation results). The parameters are not estimated

In Figure 15 the comparison between [27] observer is shown. The rotor speed in backstepping observer is precisely estimated than Krzeminski's speed observer. The control system with load torque estimation according to the (65) expression was used. The backstepping speed observer can estimate with very small error the rotor angular speed at low speeds. The motor load torque estimation improves the control system properties at zero or very low rotor speeds.

In Figure 16 stator and rotor resistance is changing in simulation. In stationary state (Fig. 17) the parameters are changing to 300% and the control system with the backstepping observer is working stable. In Figure 16 motor start up to 1.0 and reversal to –1.0 is shown – the parameters are change to 150%. If the parameters were above 200% in dynamic state the control system and the observer have variables oscillation.

The performance results for 160 kW machine were shown when (in experimental realization) the resistances of IM (R_s was changed about 30% after 5 hours work – standard technical test) and (R_r – too) – small oscillations are seen in Figure 12 (x_{12} and x_{22}) only. The serious study on parameter sensitivity exceed of volume of this paper.

9. Conclusion

The paper presents the control system of an induction machine supplied from a voltage source converter. The multiscalar backstepping control was used both in the voltage source rectifier and machine converter. The proposed control system structure is an innovative solution and it guarantees good voltage stabilization in the dc-link, which can be seen in Figure 10-11. The multiscalar backstepping control ensures good static and dynamic properties of the drive system.

The proposed method of limiting the reference variables and load torque estimation may be used in the experimental systems. The drive systems where the reference variables are not limited or are indirectly limited by the delay element are not suitable for use in the industrial drive systems.

Table 1. The motor driver system parameters

Parameter	Value
P_n (motor power)	160 kW
U_n (phase to phase voltage)	400 V
I_n (current)	279 A
J (interia)	0.045 kgm^2
n_n (rotor speed)	1500 rpm
Parameter	Per unit values
R_s (stator resist.) R_r (rotor resist.) L_m (mutual-flux induct.) L_s (stator induct.) L_r (rotor induct.)	0.01 0.012 2.15 2.205 2.205
VSC	Per unit / SI
C (capacitor in dc-link) R (inductor resist.) L (input inductor)	1.44 (4.2 mF) 0.48 (0.4 Ω) 0.098 (0.256 mH)

Table 2. Definition of per unit values

Definition	Description
$U_b = \sqrt{3}U_n$	base voltage
$I_b = I_n$	base current
$z_b = U_b / I_b$	base impedance

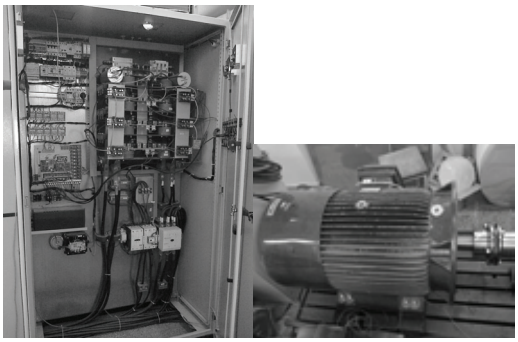

Fig. 18. 160 kW voltage source converter with induction machine

References

[1] Young Ho Hwang, Ki Kwang Park, Hai Won Yang, *Robust adaptive backstepping control for efficiency optimization of induction motors with uncertainties.* ISIE (2008).

[2] Lie Xu, Dawei Zhi, Liangzhong Yao, *Direct Power Control of Grid Connected Voltage Source Converters.* IEEE Power Engineering Society General Meeting (2007).

[3] Ramos C., Martins A., Carvalho A., *A new approach to design high performance current controllers for grid connected voltage source converters.* EPE (2009).

[4] Antoniewicz P., Kazmierkowski M.P., *Virtual-Flux-Based Predictive Direct Power Control of AC/DC Converters with Online Inductance Estimation.* IEEE Trans. on Industrial Electr. 55(12), (2008).

[5] Zanchetta P., Gerry D.B., Monopoli V.G., Clare J.C., Wheeler P.W., *Predictive current control for multilevel active rectifiers with reduced Switching frequency.* IEEE Trans. on Industrial Electr. 55(1) (2008).

[6] Borisov K., Ginn H.L., *Multifunctional VSC Based on a Novel Fortescue Reference Signal Generator.* IEEE Trans. on Industrial Electr. 57 (2009).

[7] Malinowski M., Kazmierkowski M.P., Hansen S. et al., *Virtual-flux-based direct power control of three-phase PWM rectifiers.* Trans. on Industrial Electr. 37(4), (2001).

[8] Aurtenechea S., Rodríguez M.A., Oyarbide E., Torrealday J.R., *Predictive control strategy for DC/AC converters based on direct power control.* IEEE Trans. on Industrial Electr. 54(3), (2007).

[9] Krzeminski Z., *Nonlinear control of induction motor*. Proceedings of the 10th IFAC World Congress, Munich (1987).

[10] Payam A.F., Dehkordi B.M., *Nonlinear sliding-mode controller for sensorless speed control of DC servo motor using adaptive backstepping observer*. 2006 International Conference on Power Electr., PEDES '06 (2006).

[11] Krstic M., Kanellakopoulos I., Kokotovic P., *Nonlinear and Adaptive Control Design*. John Wiley & Sons (1995).

[12] Tan H., Chang J., *Adaptive Backstepping control of induction motor with uncertainties.* Proc. the American control conference, California, pp. 1-5 (1999).

[13] Adamowicz M., Guzinski J., *Minimum-time minimum-loss speed sensorless control of induction motors under nonlinear control.* Compatibility in Power Electronics (2005).

[14] Elmaguiri O., Giri F., *Digital backstepping control of induction motors.* IEEE International Symposium on Industrial Electronics, pp. 221-226 (2007).

[15] Nemmour A.L., Mehazzem F., Khezzar A., et al., *Nonlinear control of induction motor based on the combined multi-scalar machine model and backstepping approach*. IECON '09, 35th Annual (2009).

[16] Robertsson A., Johansson R., *Observer Backstepping and Control Design of Linear Systems*. Proceedings of the 37th IEEE Conference on Decision & Control Tampa, Florida (1998).

[17] Drid S., Tadjineand M.M.-S. Naït-Saïd, *Robust backstepping vector control for the doubly fed induction motor.* IET Control Theory Appl. 1 (4), pp. 861-868 (2007).
[18] Hsin-Jang S., Kuo-Kai S., *Nonlinear Sliding-Mode Torque Control with Adaptive Backstepping Approach*. IEEE Trans. on Indust. Electronics 46(2), (1999).
[19] Hajian M., Soltani J., Markadeh G.A., Hosseinnia S., *Adaptive Nonlinear Direct Torque Control of Sensorless IM Drives With Efficiency Optimization.* IEEE Trans. on Indust. Electronics 57(3), (2010).
[20] Uddin M.N., Nam S.W., *Development and Implementation of a Nonlinear-Controller-Based IM Drive Incorporating Iron Loss With Parameter Uncertainties.* IEEE Trans. on Indust. Electronics 56(4), (2009).
[21] Lin Chih-Min, Hsu Chun-Fei, *Recurrent-Neural-Network-Based Adaptive-Backstepping Control for Induction Servo motors.* IEEE Trans. on Indust. Electronics 52(6), (2005).
[22] Tan Y., Chang J., Tan H., *Adaptive Backstepping Control and Friction Compensation for AC Servo With Inertia and Load Uncertainties.* IEEE Trans. on Indust. Electronics 50(5), (2003).
[23] Lin Faa-Jeng, Chang Chih-Kai, Huang Po-Kai, *FPGA-Based Adaptive Backstepping Sliding-Mode Control for Linear Induction Motor Drive.* IEEE Trans. on Power Electr. 22(4), (2007).
[24] Carroll J.J., Dawson D.M., *Integrator backstepping techniques for the tracking control of permanent magnet brush DC motors.* IEEE Trans. On Indust. Appl. 31(2), (1995).
[25] Trabelsi R., Kheder A., Mimouni M.F., M'sahli F., *Backstepping control for an induction motor with an adaptive Backstepping rotor flux observer.* Conf. on Control & Automation 18th MED (2010).
[26] Uddin M.N., Nam S.W., *Development and Implementation of a Nonlinear-Controller-Based IM Drive Incorporating Iron Loss With Parameter Uncertainties,* IEEE Trans. on Indust. Electronics 56(4), (2009).
[27] Krzeminski Z., *A new speed observer for control system of induction motor.* IEEE Int. Conference on Power Electronics and Drive Systems, PESC'99, Hong Kong (1999).
[28] Morawiec M., *Application of the state observer to identify squire-cage induction machine.* Przegląd Elektrotechniczny (Electrical Review) ISSN 0033-2097, 87(3), (2011).